3D Osteoconductive Composite for the Management of Large Bone Defects

Adil Akkouch[1-2], Kunal Ranat[2], Shaan Manawar[1], Liu Hong[3]

[1]Department of Orthopaedic Surgery, Medical Engineering Program,
[2]Western Michigan University Homer Stryker M.D. School of Medicine, Kalamazoo, MI
[3]Iowa Institute for Oral Health Research, College of Dentistry, The University of Iowa, Iowa City, IA

Introduction

Bone nonunions resulting from trauma, congenital abnormalities, or cancer resection are major medical concerns. A plethora of studies have reported considerable shortcomings of current clinical treatments using autografts, allografts and xenografts (1). Tissue engineering (TE) has emerged as a highly promising alternative to conventional treatment strategies for the repair or replacement of damaged bone (2). TE applications commonly encompass the use of three-dimensional (3D) scaffolds for the incorporation of cells or biomolecules. Various techniques have been used for the fabrication of 3D scaffolds (3). Generally, conventional fabrication techniques do not enable the fabrication of complex architectures. However, 3D printing enables the process of a broad range of materials and the fabrication of scaffolds with improved design and complicated 3D microstructures (4).

The purpose of the present study is to design a nontoxic and osteoconductive composite scaffold using 3D bioprinting and to evaluate bone healing in a large critical-sized calvarial defect using rat model.

Materials and Methods

Ink formulation and 3D printing

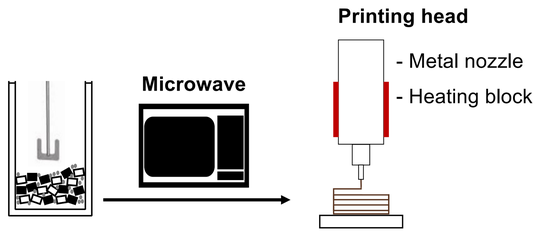

- Nanohydroxyapatite (nHA)
- Poly(DL-Lactide-co-Glycolide (PLGA)
- Polycaprolactone (PCL)

AxoDual 3D bioprinter

Printing parameters	Value
Nozzle diameter	400 µm
Extrusion temperature	190 °C
Build plate temperature	RT
Deposition speed	0.6 mm/s
Layer height	350 µm
Fiber spacing	250 µm
Infill pattern	Zig Zag 90º

Scaffolds Characterization

- Morphology: scanning electron microscopy.
- Chemical composition: Energy-dispersive X-ray spectroscopy.
- Porosity and pore size: microcomputed tomography.
- Surface wettability: water contact angle.
- Cytotoxicity and osteogenic differentiation: human bone marrow stem cell (hBMSC).
- In vivo rat critical sized-bone defect size: 11 mm.
- Bone formation: Histology (H&E) and microCT analysis (BV/TV & Bone mineral density (BMD).

Results

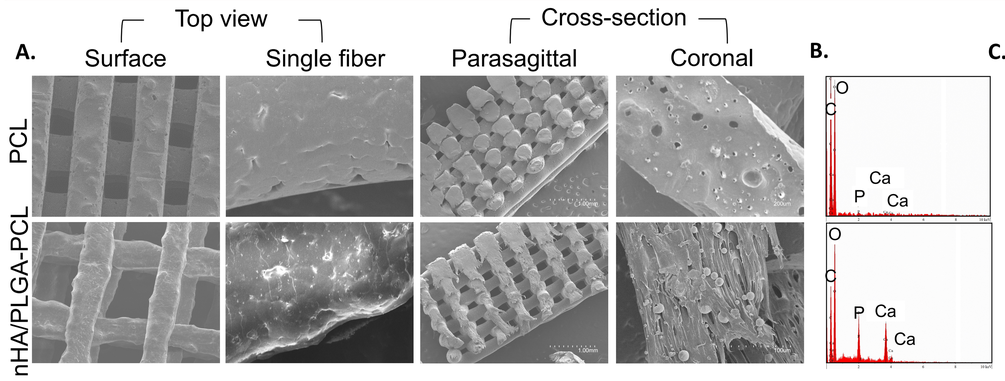

	Fiber diameter (µm)	Fiber spacing (µm)	Density (mg/cm³)	Porosity (%)	Contact angle (º)
PCL	349.13 ± 11.30	245.06 ± 7.96	0.57 ± 0.05	50.38 ± 4.44	103.88 ± 2.14
nHA/PLGA-PCL	315.34 ± 21.36	278.41 ± 19.95	0.50 ± 0.06	53.46 ± 5.53	73.87 ± 1.92

Figure 1. Morphological and physicochemical characterization of the 3D printed scaffolds.
A. SEM micrographs of the 3D printed scaffolds. nHA/PLGA/PCL scaffolds displayed a high uniform porosity and highly interconnected pores. Cross-section of individual fiber confirmed the presence of nHA within the nHA/PLGA-PCL fibers.
B. Surface analysis revealed the presence of calcium and phosphorous ions in the nHA/PLGA-PCL scaffolds.
C. The chemical composition of the ink led to differences among the printed scaffolds in terms of fiber diameter, spacing, density and total porosity. nHA/PLGA-PCL scaffolds presented higher hydrophilicity when compared to highly hydrophobic PCL.

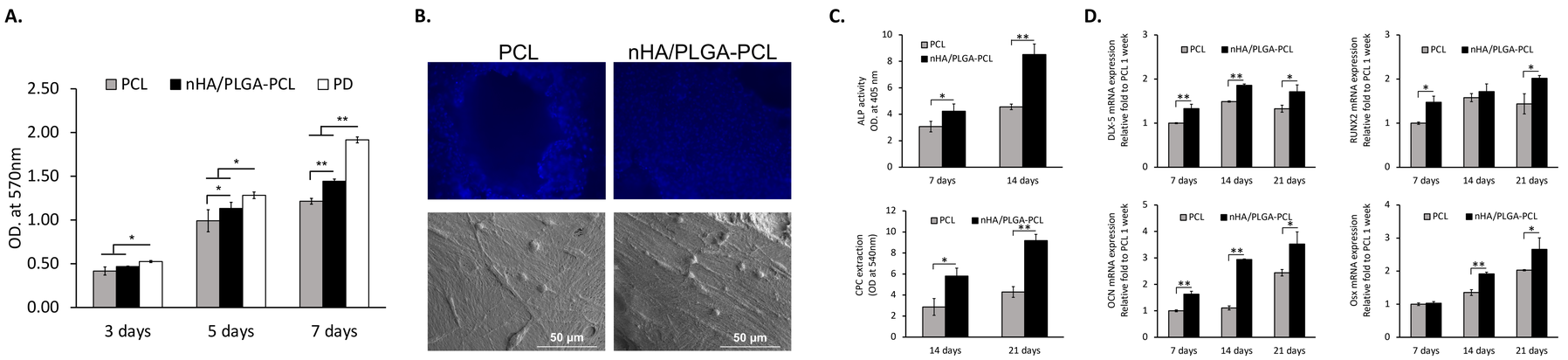

Figure 2. 3D printed nHA/PLGA-PCL scaffolds enhance adhesion, proliferation and osteogenic differentiation of hBMSCs in vitro. Printed scaffolds (11 x 11 x 2 mm), were loaded with $5x10^5$ hBMSCs and cultured in osteogenic medium for various periods.
A. hBMSCS metabolic activity was evaluated by MTT.
B. hBMSCs were cultured on scaffolds for 1 day then visualized using fluorescence microscopy (stained with DAPI) or using SEM.
C. Quantitative measurement of ALP activity (Alkaline phosphatase) in hBMSCs cultured on 3D printed scaffolds, 7 and 14 days after exposure to osteogenic differentiation medium**.** hBMSCs mineralization assessed using Alizarin red staining (ARS) and cetylpyridinium chloride (CPC) extraction method, 14 and 21 days after osteogenic differentiation.
D. Gene expression of osteoblast-specific transcription factors and differentiation markers: DLX-5 (Distal-Less Homeobox 5), RUNX2 (Runt-Related Transcription Factor 2), OCN (Osteocalcin) and Osx (Osterix) 7, 14 and 21 days after exposure to osteogenic differentiation medium. *:p < 0.05; **: p < 0.01; n=3.

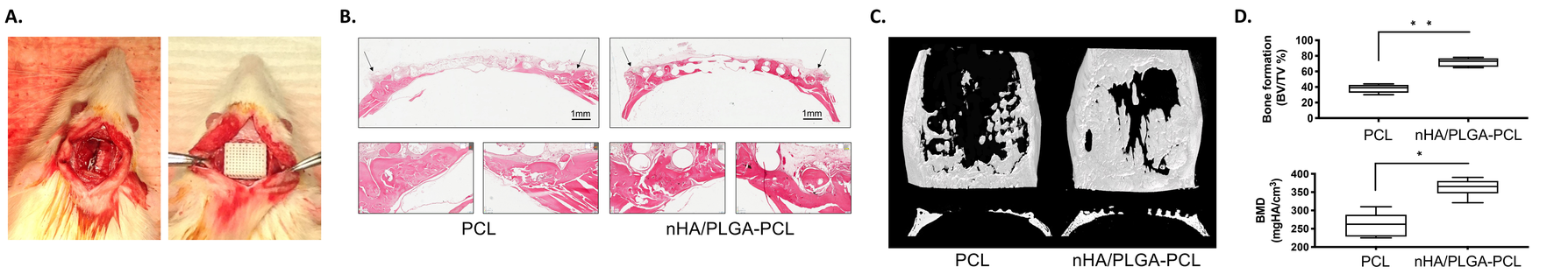

Figure 3. 3D printed nHA/PLGA-PCL scaffolds promote bone regeneration in large-scale calvarial defects.
A. Under general anesthesia, full-thickness defects measuring 11 x 11 mm were created in the parietal bones with attention paid to preserving the dura mater.
B. The 3D printed scaffolds were then inserted into the defects. After 12 weeks, animals were euthanized, and bone formation was examined using Hematoxylin and Eosin (H&E) staining (coronal-section perpendicular to the sagittal suture through the center of the defect), and
C. microCT (top-view and cross-section images).
D. Bone volume fraction (BV/TV) and bone mineral density (BMD) were used to calculate new bone formation within an ROI of 10-mm from the center of the defects. The microCT threshold was first calibrated and then applied to all samples. *:p < 0.05; **: p < 0.01; n = 6.

Conclusion

We produced a bioactive and osteoconductive scaffold using 3D printing technology with high osteogenic potential for large bone fracture repair. This scaffold may be useful as patient-specific implant for guided bone regeneration in clinical setting.

References

1. Akkouch A. et al. Hum Gene Ther. 2019.
2. Akkouch A et al. J Biomater Appl. 2014.
3. Loh. et al., Tissue Eng Part B Rev, 2013.
4. Matai I, et al. Biomaterials 2020.

Acknowledgments

This study was supported by the NIDCR R01 DE026433, and the Startup funds from Western Michigan University Homer Stryker M.D. School of Medicine.